Effect of Ionospheric Variability on the Electron Energy Spectrum produced from Incoherent Scatter Radar Measurements

Oliver Stalder, Björn Gustavsson

February 27, 2023

Abstract

The ionospheric composition is modeled for the relevant species at 80 - 150 km during auroral precipitation. The model is combined with the ElSpec algorithm [4] to produce differential energy spectrum from incoherent scatter radar measurements. The impact of ionospheric variability on the inversion is shown. We find up to ... % deviations in the differential energy spectrum and up to ...% deviation in field aligned current compared to a constant ionosphere model.

1 Introduction

Ion density variations in the ionosphere can significantly influence the recombination time of electrons. This has direct influence on inversion techniques that use electron density profiles to infer differential energy spectra of electrons precipitating during aurora.
Electron density inversion makes use the electron continuity equation:

$$\frac{dn_e}{dt} = q_e - \alpha_{eff} n_e^2 + \nabla \cdot (n_e \mathbf{v}) \tag{1.1}$$

with n_e being the electron density, q the production and α_{eff} the effective recombination rate. The convective term $n_e\mathbf{v}$ is usually neglected due to the lack of information on the velocity. Transport and ionization of electrons precipitating in the ionosphere are governed by a set of linear differential equations, allowing to formulate the production height profile as a matrix product with a discretized differential energy flux ϕ:

$$q_e = A\phi \tag{1.2}$$

with A representing the production rates at discrete energies and altitudes [1, 3]. If the effective recombination rate is assumed constant, the problem is largely independent from ion densities. However, the recombination rate depends on the ion densities:

$$\alpha_{eff} = \alpha_{\mathrm{NO}^+,e} \frac{n_{\mathrm{NO}^+}}{n_e} + \alpha_{\mathrm{O}_2^+,e} \frac{n_{\mathrm{O}_2^+}}{n_e} \tag{1.3}$$

It has been shown that the ionospheric composition varies greatly during auroral precipitation [2] and it is assumed to have a considerable effect on electron inversion techniques [4]. This is the first study, to the author's knowledge, that takes the dynamic variability into account by modeling the relevant ion and minor species densities.

2 Method

To model the ionospheric composition in response to the precipitation, the coupled continuity equations for minor neutral and in species (H, H+, N(4S), N(2D), N+, N2+, NO, NO+, O(1D), O(1S),

Reaction	Rate $[m^{-3}s^{-1}]$	Branching ratio
$O_2^+ + e^- \longrightarrow O(1D) + O(1S) + O$	$\alpha_1 = 1.9 \times 10^{-13}\,(T_e/300)^{-0.50}$	1.20, 0.10, 0.70
$N_2^+ + e^- \longrightarrow N(2D) + N(4S)$	$\alpha_2 = 1.8 \times 10^{-13}\,(T_e/300)^{-0.39}$	1.90, 0.10
$NO^+ + e^- \longrightarrow O + N(2D) + N(4S)$	$\alpha_3 = 4.2 \times 10^{-13}\,(T_e/300)^{-0.85}$	1.00, 0.78, 0.22
$N(4S) + O_2 \longrightarrow NO + O$	$\beta_1 = 4.4 \times 10^{-18}\,\exp(-3220/T_n)$	
$N(2D) + O_2 \longrightarrow NO + O(1D) + O$	$\beta_2 = 5.3 \times 10^{-18}$	1.00, 0.10, 0.90
$N(4S) + NO \longrightarrow N_2 + O$	$\beta_4 = 1.5 \times 10^{-18}\,T_n^{0.50}$	
$N(2D) + O \longrightarrow N(4S) + O$	$\beta_5 = 2.0 \times 10^{-18}$	
$N(2D) + e^- \longrightarrow N(4S) + e^-$	$\beta_6 = 5.5 \times 10^{-16}\,(T_e/300)^{0.5}$	
$N(2D) + NO \longrightarrow N_2 + O$	$\beta_7 = 7.0 \times 10^{-17}$	
$O^+(4S) + N_2 \longrightarrow NO^+ + N(4S)$	$\gamma_1 = \begin{cases} 5 \times 10^{-19} & T \le 1000 \\ 4.5 \times 10^{-20}\,(T/300)^2 & T > 1000 \end{cases}$	
$O^+(4S) + O_2 \longrightarrow O_2^+ + O$	$\gamma_2 = 2.0 \times 10^{-17}\,(T_r/300)^{-0.40}$	
$N_2^+ + O \longrightarrow NO^+ + N(2D)$	$\gamma_4 = 1.4 \times 10^{-16}\,(T_r/300)^{-0.44}$	
$N_2^+ + O_2 \longrightarrow O_2^+ + N_2$	$\gamma_5 = 5.0 \times 10^{-17}\,(T_r/300)^{-0.80}$	
$O_2^+ + N_2 \longrightarrow NO^+ + NO$	$\gamma_8 = 5.0 \times 10^{-22}$	
$N^+ + O_2 \longrightarrow NO^+ + O + O(1D)$	$\gamma_{10} = 2.6 \times 10^{-16}$	1.00, 0.30, 0.70
$N^+ + O_2 \longrightarrow O_2^+ + N(4S)$	$\gamma_{11} = 1.1 \times 10^{-16}$	
$O^+(4S) + H \longrightarrow H^+ + O$	$\gamma_{12} = 6.0 \times 10^{-16}$	
$O_2^+ + NO \longrightarrow NO^+ + O_2$	$\gamma_{15} = 4.4 \times 10^{-16}$	
$O_2^+ + N(4S) \longrightarrow NO^+ + O$	$\gamma_{16} = 1.8 \times 10^{-16}$	
$O_2^+ + N(2D) \longrightarrow N^+ + O_2$	$\gamma_{17} = 2.5 \times 10^{-16}$	
$N_2^+ + NO \longrightarrow NO^+ + N_2$	$\gamma_{18} = 3.3 \times 10^{-16}$	
$N_2^+ + O \longrightarrow O^+(4S) + N_2$	$\gamma_{19} = 1.4 \times 10^{-16}\,(T_r/300)^{-0.44}$	
$H^+ + O \longrightarrow O^+(4S) + H$	$\gamma_{20} = (8/9)\gamma_{12}\sqrt{\frac{Ti+T_n/4}{T_n+Ti/16}}$	
$O^+(4S) + NO \longrightarrow NO^+ + O$	$\gamma_{21} = 8.0 \times 10^{-19}$	
$O^+(4S) + N(2D) \longrightarrow N^+ + O$	$\gamma_{26} = 1.3 \times 10^{-16}$	
$N^+ + O_2 \longrightarrow O^+(4S) + NO$	$\gamma_{27} = 3.0 \times 10^{-17}$	
$N^+ + O \longrightarrow O^+(4S) + N(4S)$	$\gamma_{28} = 5.0 \times 10^{-19}$	
$N^+ + H \longrightarrow H^+ + N(4S)$	$\gamma_{29} = 3.6 \times 10^{-18}$	
$N^+ + O_2 \longrightarrow O_2^+ + N(2D)$	$\gamma_{33} = 2.0 \times 10^{-16}$	

Tab. 2.1: Chemical reactions in the E-region and reaction rates.

O+(4S), O2+) are integrated in time:

$$\frac{dn_k}{dt} = q_k - l_k \tag{2.1}$$

$$n_k(t) = n_k(t_0) + \int_{t_0}^{t} \frac{dn_k}{dt} dt \tag{2.2}$$

where production and loss terms are of the form $q_k = \sum_{i,j\to k} \alpha_{ij} n_i n_j$ and $l_k = -\sum_{i,k} \alpha_{ik} n_i n_k$, summed over all relevant reactions. Table 2.1 shows the reactions and reaction rates taken into account. In addition, ionization of major neutral species from electron precipitation is accounted for:

$$q_{A,O^+} = q_e \frac{0.56\, n_O}{0.92\, n_{N_2} + n_{O_2} + 0.56\, n_O} \tag{2.3}$$

$$q_{A,N_2^+} = q_e \frac{0.92\, n_{N_2}}{0.92\, n_{N_2} + n_{O_2} + 0.56\, n_O} \tag{2.4}$$

$$q_{A,O_2^+} = q_e \frac{n_{O_2}}{0.92\, n_{N_2} + n_{O_2} + 0.56\, n_O} \tag{2.5}$$

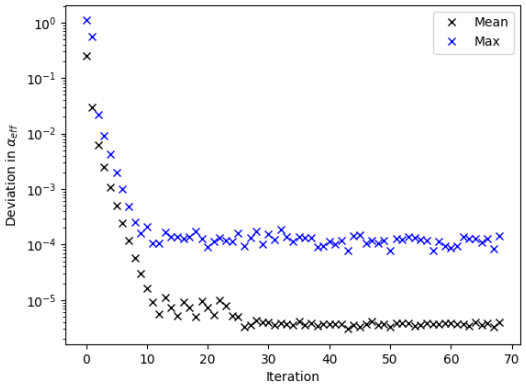

Fig. 3.1: The sum of absolute changes in the effective recombination rate is shown.

Inverting the electron density height profiles to differential energy spectra is performed with the ElSPec algorithm [4], extended by a robust statistics implementation [B. Gustavsson, unpublished]. The implementation of ElSPec used requires the entire data set to be processed at once. Therefore, instead of combining the ion chemistry model at each timestep with ElSpec, an iterative approach is adopted: The ElSpec algorithm is started with an assumed ionospheric composition, producing an electron production q_e model in altitude and time. This is then used in the ion chemistry model to track the evolution of ionospheric composition, and given as an input into the next iteration of ElSpec. Over few iterations, the ionospheric composition is converging to negligibly small deviations in between iterations. Furthermore, a 30 minute time window was added at the start. A constant electron production is assumed, equal to the production of the first step in the time series. This allows the model ionosphere to reach an equilibrium state that is more realistic than the assumed composition. Lastly, deviations in densities are damped by a factor of 2 between iterations to suppress oscillations.

3 Results

A data set from the 12th of December 2006, recorded with the EISCAT UHF radar in Tromsø is analyzed. First, the convergence of this approach is tested. Figure 3.1 shows the mean relative deviation in the effective recombination rate compared to the last iteration, and the maximum relative deviation. There is a clear convergence until the 10th iteration.

Figure 3.2 shows a comparison between the inversion results obtained with a non-variable and variable ionosphere.

References

[1] Xiaohua Fang et al. "Parameterization of monoenergetic electron impact ionization". en. In: *Geophysical Research Letters* 37.22 (2010). _eprint: https://onlinelibrary.wiley.com/doi/pdf/10.1029/2010GL045406. ISSN: 1944-8007. DOI: 10.1029/2010GL045406. URL: https://onlinelibrary.wiley.com/doi/abs/10.1029/2010GL045406 (visited on 05/30/2022).

[2] R. A. Jones and M. H. Rees. "Time dependent studies of the aurora—I. Ion density and composition". en. In: *Planetary and Space Science* 21.4 (Apr. 1973), pp. 537–557. ISSN: 0032-0633. DOI: 10.1016/0032-0633(73)90069-X. URL: https://www.sciencedirect.com/science/article/pii/003206337390069X (visited on 09/22/2022).

[3] Joshua Semeter and Farzad Kamalabadi. "Determination of primary electron spectra from incoherent scatter radar measurements of the auroral E region". en. In: *Radio Science* 40.2 (2005). _eprint: https://onlinelibrary.wiley.com/doi/pdf/10.1029/2004RS003042. ISSN: 1944-799X. DOI: 10.1029/2004RS003042. URL: https://onlinelibrary.wiley.com/doi/abs/10.1029/2004RS003042 (visited on 05/02/2022).

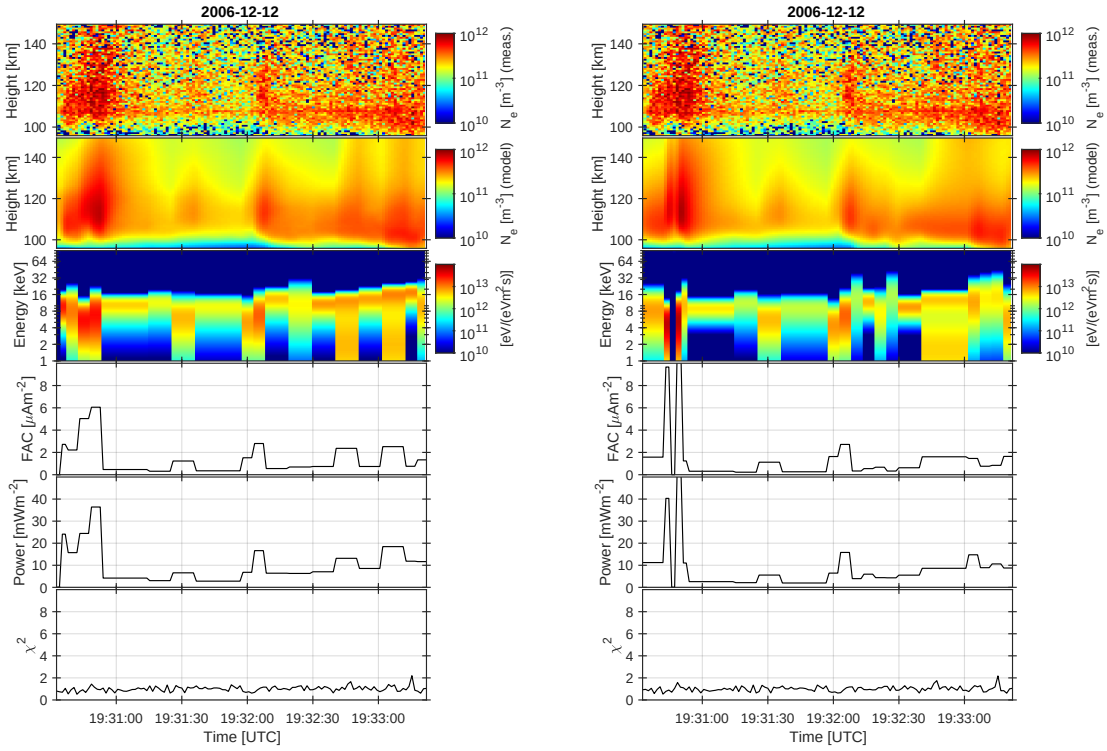

a b

Fig. 3.2: ElSpec results with (a) constant ionospheric densities and (b) variable ionospheric densities.

[4] Ilkka I. Virtanen et al. “Electron Energy Spectrum and Auroral Power Estimation From Incoherent Scatter Radar Measurements”. en. In: *Journal of Geophysical Research: Space Physics* 123.8 (2018). _eprint: https://onlinelibrary.wiley.com/doi/pdf/10.1029/2018JA025636, pp. 6865–6887. ISSN: 2169-9402. DOI: 10.1029/2018JA025636. URL: https://onlinelibrary.wiley.com/doi/abs/10.1029/2018JA025636 (visited on 04/21/2022).